Chemical Engineering Journal 147 (2009) 6–12

Contents lists available at ScienceDirect

Chemical Engineering Journal

journal homepage: www.elsevier.com/locate/cej

Small-angle neutron scattering studies of model protein denaturation in aqueous solutions of the ionic liquid 1-butyl-3-methylimidazolium chloride

Gary A. Baker[a,*], William T. Heller[a,b,*,1]

[a] Chemical Sciences Division, Oak Ridge National Laboratory, Oak Ridge, TN 37831, USA
[b] Center for Structural Molecular Biology, Oak Ridge National Laboratory, Oak Ridge, TN 37831, USA

ARTICLE INFO

Keywords:
Ionic liquids
Protein aggregation
Small-angle scattering
Chaotropes
Cytochrome *c*
Human serum albumin
Hofmeister series

ABSTRACT

As we advance our understanding, ionic liquids (ILs) are finding ever broader scope within the chemical sciences including, most recently, pharmaceutical, enzymatic, and bioanalytical applications. With examples of enzymatic activity reported in both neat ILs and in IL/water mixtures, enzymes are frequently assumed to adopt a quasi-native conformation, even if little work has been carried out to date toward characterizing the conformation, dynamics, active-site perturbation, cooperativity of unfolding transitions, free energy of stabilization, or aggregation/oligomerization state of enzymes in the presence of an IL solvent component. In this study, human serum albumin and equine heart cytochrome *c* were characterized in aqueous solutions of the fully water-miscible IL 1-butyl-3-methylimidazolium chloride, [bmim]Cl, by small-angle neutron and X-ray scattering. At [bmim]Cl concentrations up to 25 vol.%, these two proteins were found to largely retain their higher-order structures whereas both proteins become highly denatured at the highest IL concentration studied here (i.e., 50 vol.% [bmim]Cl). The response of these proteins to [bmim]Cl is analogous to their behavior in the widely studied denaturants guanidine hydrochloride and urea which similarly lead to random coil conformations at excessive molar concentrations. Interestingly, human serum albumin dimerizes in response to [bmim]Cl, whereas cytochrome *c* remains predominantly in monomeric form. These results have important implications for enzymatic studies in aqueous IL media, as they suggest a facile pathway through which biocatalytic activity can be altered in these nascent and potentially green electrolyte systems.

Published by Elsevier B.V.

1. Introduction

The implementation of biomolecules in ionic liquid (IL)-based media has sparked immense interest for applications ranging from applied biocatalysis for hydrogen production to bioanalysis and cellulose processing [1–3], resulting in several reviews on the subject [3–12]. Lipases, most notably *Candida antarctica* lipase B (CALB), have received the most attention [13–29], due primarily to their broad industrial utility as well as for exceptional tolerance of non-aqueous environments; much of the research to date has focused solely on enzymatic activity. Other proteins have also been characterized for their catalytic activity, including α-chymotrypsin [30,31], horseradish peroxidase [32–34], papain [35,36], cytochromes [37–39] and tyrosinase [40], among others. Most recently, the first examples of homogeneous and heterogeneous bioreceptor-based immunoassay were described in which an antibody was found to retain its high-affinity haptenic recognition in aqueous buffer containing 75 vol.% [bmim][BF_4] as well as in a number of water-free [bmim][A] ILs where A = BF_4^-, NTf_2^-, TfO^-, or PF_6^- [41]. The excitement about possible application of enzymatic transformations and clean biotechnological processes by means of IL-based media continues to drive research in this area; in this regard, ILs may be employed as co-solvents for water, in biphasic systems, or as "neat" solvents containing little or no water. The effects of various ILs on enzymatic reactions, however, vary wildly and unpredictably, sometimes with seemingly conflicting reports. Clearly, a profusion of systematic studies are mandatory in order to establish a general understanding of structure–function relationships for enzymes in IL media.

Information on protein structure, dynamics, and solvation is crucial for understanding protein function in ILs. Regardless, relatively few biophysical characterizations of protein molecules in systems containing ILs exist in the literature. In particular, the influence of ILs on enzyme structure has only recently become a focus of study. In the original report on protein spectroscopy conducted within an IL, it was shown, using fluorescence from the single tryptophan residue in the sweet protein monellin, that the use of the IL 1-butyl-1-methylpyrrolidinium bis(trifluoromethylsulfonyl)imide,

* Corresponding author. Tel.: +1 865 241 9361; fax: +1 865 576 5235.
E-mail addresses: bakerga1@ornl.gov (G.A. Baker), hellerwt@ornl.gov (W.T. Heller).
[1] Tel.: +1 865 241 0093; fax: +1 865 574 6268.

1385-8947/$ – see front matter. Published by Elsevier B.V.
doi:10.1016/j.cej.2008.11.033

[bmpy][NTf_2], containing a modest amount of water (2 vol.%) yielded an astonishing entropically driven stabilization in opposition to thermal unfolding (i.e., the unfolding entropy, ΔS°, was determined to be 250 and 136 $J K^{-1} mol^{-1}$ for monellin in water and [bmpy][NTf_2] containing 2 vol.% water, respectively), consistent with the more rigid solvation present within wet [bmpy][NTf_2] [42]. Second-derivative single-pass attenuated total reflection Fourier transform infrared (ATR-FTIR) spectroscopy in the amide I region was employed by Lou et al. [36] to reveal the impact of the presence of 15 vol.% 1-alkyl-3-methylimidazolium, [$C_n$mim]$^+$, ILs combined with various anions on the structure of papain in buffer, and to correlate these conformational changes with the observed catalytic activity and selectivity of the enzyme. Contributing to the prevailing outlook in this area, their results demonstrate that in aqueous IL systems involving anions with pronounced hydrogen bond basicity (i.e., $[Cl]^-$, $[NO_3]^-$, $[CH_3CO_2]^-$, and especially $[HSO_4]^-$), a non-native amide I spectrum was observed as a result of disruption of internal hydrogen bonding, this perturbation being accompanied by a proportionate loss of activity. Meanwhile, for the more enzyme-suited anion $[BF_4]^-$, which exhibits a lower nucleophilicity, comparable or higher activity and enantioselectivity was exhibited by papain in comparison with aqueous phosphate buffer. Additionally, it is notable that although losses in α-helical content were apparent for papain in aqueous [$C_n$mim][BF_4] (n = 2–6), the contribution of β-turns and sheets increased, this evolution in secondary structure ostensibly leading to a more compact and stable enzyme configuration. Similarly, Iborra and co-workers [43] reported that the stabilization of CALB observed both in 1-ethyl-3-methylimidazolium bis(trifluoromethylsulfonyl)imide, [emim][NTf_2], and butyltrimethylammonium bis(trifluoromethylsulfonyl)imide, [N_{4111}][NTf_2], at 2 vol.% water content and 50 °C, was associated with a partial preservation of native α-helicity with simultaneous enhancement in β-strand content (as determined by circular dichroism, CD), again presumably resulting in a more condensed enzyme conformation displaying catalytic activity. In a prior study, the same authors showed that [emim][NTf_2] containing 12.5 vol.% 1-propanol bestowed excellent thermal stability to α-chymotrypsin, with an unfolding enthalpy triple that determined in water [44]; once more, the degree of stabilization appeared to be linked to the prevalence of β-strands in the presence of IL. Using small-angle neutron scattering (SANS) and dynamic light scattering (DLS), Sate et al. [45] showed that CALB dissolved in [emim][A] ILs undergoes substantial and inhomogeneous agglutination leading to a curtailed activity (A = $EtOSO_3^-$ and NO_3^-) or complete deactivation (A = $N(CN)_2^-$), lending credence to the notion that highly coordinating anions do not support enzyme action in ILs. In a key study, Weingärtner used differential scanning calorimetry (DSC) to systematically elucidate the impact of various cation/anion pairings on the thermal stability of ribonuclease A in aqueous systems containing a range of [emim]$^+$ or bromide-based ILs based on salt-induced shifts of the transition temperature [46]. During this research, the authors learned that protein–IL interactions within aqueous solutions can be loosely interpreted within a Hofmeister framework and, consistent with enzyme activity results from Zhao [47], anion variations generally appear to have larger consequences than cation variations. Incidentally, it is likely that this rule of thumb represents something of an oversimplification, particularly as ILs including wider cation types become available [48]. Most recently, fluorescence spectroscopic examination of singly-labeled defatted human serum albumin (HSA), prepared by site-specific conjugation of the solvent-responsive fluorescent reporter acrylodan to Cys-34, revealed that the thermal unfolding process of HSA in three different 1-butyl-3-methylimidazolium-based ILs ([bmim][A]; A = NTf_2^-, BF_4^-, and PF_6^-), as well as the protein's dynamical motions, deviated markedly from the mechanism followed in aqueous buffer [49]. The Angell group [50] also recently reported a remarkable multi-year stabilization against aggregation losses for near-saturation solutions of lysozyme in IL-rich, ice-avoiding solvent systems also containing sucrose and water. The protic IL ethylammonium nitrate itself was found to confer protection against aggregation; indeed, ~97% retention in refoldable protein sample per denaturing cycle was established, as judged by the declining area under the unfolding endotherm in successive DSC upscans to 100 °C. The vast array of physicochemical properties afforded by ILs necessitates continued research in this area to build a more complete picture of the influence of IL ion pairing on protein structure and aggregation and to correlate this behavior with enzyme activity.

Small-angle scattering methods, using neutrons or X-rays (SANS and SAXS, respectively), are ideally suited to the study of the impact of ILs on the structures of soluble proteins. These methods probe the global conformations of particles in solution, and have been used extensively to study biological macromolecules in solution; a review emphasizing this topic appeared recently by Svergun and Koch [51]. SANS and SAXS are excellent probes of solution-phase protein structural modification (e.g., denaturation, aggregation, oligomerization, ligand complexation), because these techniques are inherently sensitive to changes in the shape, size, and compactness of the scattering particle. In particular, a fair number of experimental studies have appeared in which small-angle scattering methods provide key information concerning the solution conformation of model proteins like the serum albumins [52–55] or equine heart cytochrome *c* (cyt *c*) [56–60] under denaturing conditions driven by chemical agents, or extremes of pH or temperature.

In the current work, we present the details of our investigations into the behavior of two of the most thoroughly characterized proteins within aqueous mixtures of the entirely water-miscible IL 1-butyl-3-methylimidazolium chloride, [bmim]Cl, using small-angle scattering and CD spectroscopy. The first model protein we selected for study, equine heart cyt *c*, is among the most well-studied metalloproteins. A class I *c*-type cytochrome involved in electron transfer in the mitochondrial respiratory chain, equine heart cyt *c* consists of a single polypeptide chain containing 104 amino acid residues that is covalently anchored by two thioether bonds at Cys-14 and Cys-17 to an iron-containing heme. The second archetypical protein we chose, HSA, is larger and a bit more complex, consisting of a single polypeptide chain of 585 amino acid residues and having a heart-shaped structure divided into three major and fairly distinct domains stabilized by 17 disulfide bonds. The most abundant protein found within human plasma, not surprisingly, HSA is involved in many physiological functions, including blood pH and pressure maintenance. Both cyt *c* and HSA were found to denature in high concentrations of [bmim]Cl, but the impact of the IL on the structure was not particularly pronounced until the aqueous solution reached 50 vol.% [bmim]Cl. SANS demonstrates a transition of the polypeptide chains from compact structures to highly denatured states; SAXS results corroborate this view. Visible CD spectroscopy in the Soret region of cyt *c* suggests that the environment of the heme is considerably perturbed at 25 vol.% [bmim]Cl before adopting a state consistent with a urea-denatured state [61] at the highest IL content studied (50 vol.%).

2. Experimental

2.1. Materials

Essential fatty acid-free human serum albumin (HSA) and cyt *c* from equine heart were obtained as lyophilized powders from Sigma (St. Louis, MO, USA) and used without further purification. High-purity [bmim]Cl was synthesized according to established lit-

erature procedures [62,63]. Stock solutions of HSA and cyt *c* for the small-angle scattering measurements were prepared by dissolving protein in 20 mM Tris buffer at pH 7.4. Prior to scattering analysis, each protein stock solution was filtered using a sterile 0.02-μm Whatman Anotop 25 syringe filter equipped with 10-mm diameter inorganic membrane (Maidstone, UK) to remove large particulates and proteinaceous aggregates. The filtered protein stock concentrations were determined by UV–vis absorption to be 9.0 and 25.1 mg/mL for HSA and cyt *c*, respectively. Samples were then diluted to half the original protein concentration using the appropriate proportion of [bmim]Cl and Tris buffer to yield protein in buffer solutions containing 0, 10, 25, and 50 vol.% [bmim]Cl. Due to the relatively high viscosity of supercooled [bmim]Cl at ambient temperature, the material was added by weight based on the measured density of the liquid phase (1.092 g cm^{-3}).

2.2. Circular dichroism measurement

Visible circular dichroism (CD) spectra (300–500 nm) were obtained at room temperature using a 1-mm path length cuvette on a JASCO J-810 spectropolarimeter (JASCO Inc., Easton, MD). Due to strong far-UV background absorption associated with [bmim]Cl, CD signals could only be dependably measured in the Soret band region centered near 410 nm for equine heart ferri-cyt *c*.

2.3. Small-angle scattering measurements

SANS data were collected within the Center for Structural Molecular Biology on the Bio-SANS instrument. Intensity patterns for samples and appropriate backgrounds were collected using a wavelength of 6 Å with a wavelength spread, $\Delta\lambda/\lambda$, of 0.15. Two sample-to-detector distances were used for the HSA measurements, namely 2 and 7 m. Cyt *c* was measured solely at the shorter distance due to the much smaller size of the protein. Additional SAXS data were collected for the proteins in 0, 10, and 50 vol.% [bmim]Cl using the Center for Structural Molecular Biology 4 m SAXS facility [64]. Both SAXS and SANS data were collected at ambient temperature (~22 °C). Scattering data were reduced using standard procedures [64] to correct for background and detector sensitivity and were azimuthally averaged to produce the unidimensional intensity profile $I(q)$ vs. q. q is the magnitude of the scattering vector and is equal to $4\pi \sin(\theta)/\lambda$ where λ is the wavelength and 2θ is the scattering angle from the incident beam.

2.4. Small-angle scattering data analysis

Data were fit for the pair distribution function, $P(r)$, which is related to the measured intensity by the following equation:

$$P(r) = \frac{1}{2\pi^2}\int_0^\infty dq(qr)I(q)\sin(qr) \quad (1)$$

The indirect Fourier transform algorithm implemented in the software GNOM [65] was used to determine $P(r)$ and the maximum linear dimension, d_{max}, from the measured intensity profiles. The fitting also provides R_g, which is the second moment of $P(r)$, and the forward scatter, $I(0)$. Comparison of the IL-free small-angle scattering data to a model intensity profile calculated from the high-resolution structure was performed using the program ORNL_SAS [66]. The forward scatter of a dilute solution of non-interacting particles is given by the following equation:

$$I(0) = N_P V_P^2(\rho_P - \rho_S)^2 \quad (2)$$

where N_P is the number of particles per unit volume, V_P is the volume of the scattering particle, ρ_P is the scattering length density of the particle and ρ_S is the scattering length density of the solvent.

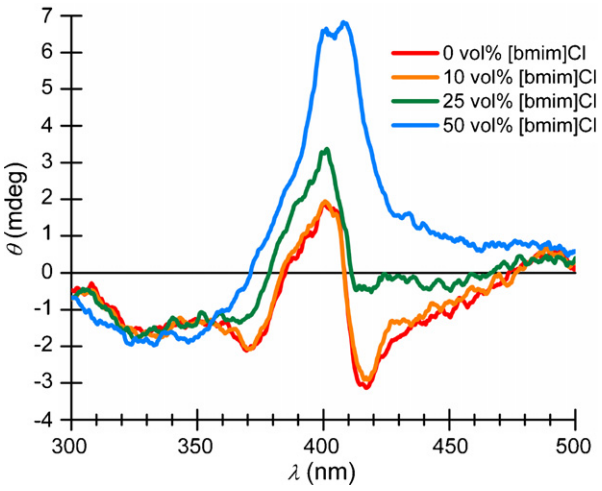

Fig. 1. Soret-region CD spectra of cyt *c* in 0, 10, 25, and 50 vol.% [bmim]Cl in 20 mM pH 7.4 Tris buffer.

The forward scatter, either in absolute units of 1 cm^{-1} or relative units if the measurements are made with the same instrument in the same configuration, provides a means of characterizing the samples for changes in the oligomerization state of the scattering particles given a known concentration.

3. Results and discussion

Visible CD spectra measured in the Soret region for equine heart cyt *c* in the aqueous [bmim]Cl mixed solvent medium are provided in Fig. 1. It can be observed that the protein shows a CD pattern in 10 vol.% [bmim]Cl that is identical, within the experimental noise, to the one seen in the aqueous phosphate buffer control, and one consistent with the previously measured Soret-region CD spectrum of native ferri-cyt *c* [61], reflecting minimal changes in the heme active-site structure in the presence of 10 vol.% [bmim]Cl. As the [bmim]Cl concentration increases to 25 vol.%, the CD spectrum is characterized by a marked decrease in the intensity of the strong negative Cotton band at 417 nm and a concomitant rise in the intensity of the positive Cotton effect near 400 nm. When the mixed solvent mixture reaches 50 vol.% [bmim]Cl (~3.1 M), the visible CD spectrum of cyt *c* no longer retains the characteristic dichroic signature of ferri-cyt *c* in aqueous solution and instead adopts a shape that is consistent with the urea-denatured state of the protein [61]. These spectroscopic changes signal a significant modification in heme–polypeptide interactions—likely an increase in the planarity of the ferric heme moiety in the mixed solvent medium—and are reminiscent of results obtained by Sivakolundu and Mabrouk [67] for ferri-cyt *c* in aqueous mixtures of acetonitrile approaching 25 vol.%. We note that the heme group of cyt *c*, which is covalently bound to the polypeptide chain, is not deeply buried [68] and, as a result, the protein structure may remain largely intact even as the local environment surrounding the heme experiences significant local perturbation.

SANS profiles collected for cyt *c* in the various aqueous mixtures of [bmim]Cl are shown in Fig. 2. SAXS data collected using our laboratory-based X-ray instrument [64] for cyt *c* (not shown) were of insufficient quality for analysis due to the small size of the protein. The electronic radius of gyration R_g and zero-angle intensity $I(0)$ parameters determined for cyt *c* in [bmim]Cl aqueous solutions from SANS measurements are summarized in Table 1, and the structure of the protein in the IL-free solution is consistent with the known crystal structure of the protein [68], as shown in Fig. 2. Pair distribution function $P(r)$ curves determined from these data are

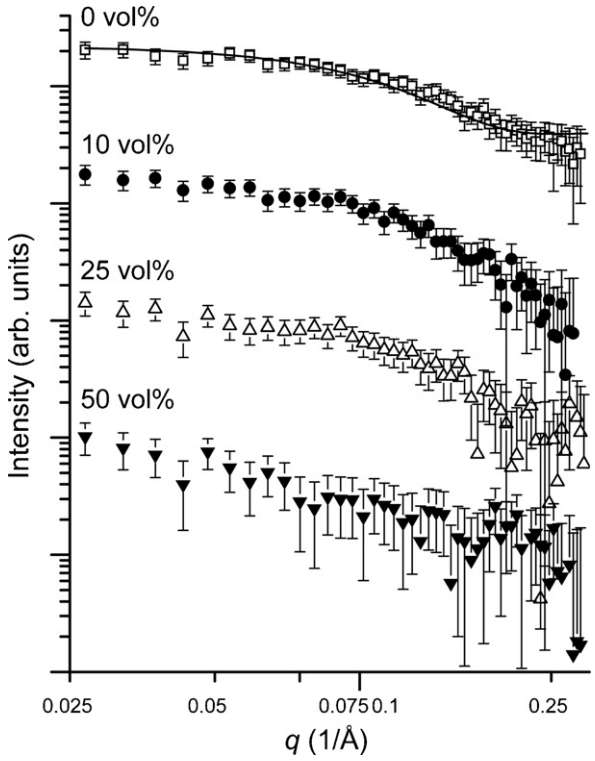

Fig. 2. SANS profiles of cyt *c* in 0, 10, 25, and 50 vol.% aqueous [bmim]Cl. The continuous solid curve shown is the model profile calculated using ORNL_SAS [66] based on the crystal structure of cyt *c* [68] (PDB ID: 1HRC). The scattering results have been offset for clarity.

Table 1
Structural parameters derived from SANS data of cyt *c*.

Vol.% [bmim]Cl	R_g (Å)	d_{max} (Å)	$I(0)/I_{0\%}(0)$ (meas.)	$I(0)/I_{0\%}(0)$ (calc.)
0	12.8 ± 0.8	40	1.00	1.00
10	14.1 ± 0.8	42	0.90 ± 0.08	0.88
25	13.0 ± 1.7	45	0.65 ± 0.10	0.71
50	28.7 ± 5.7	90	0.55 ± 0.23	0.46

given in Fig. 3. The effect of the IL on the cyt *c* structure is relatively small at 10 and 25 vol.%, resulting in only slight increases in R_g and d_{max}. The main peak of $P(r)$ shifts to lower distances with the addition of up to 25 vol.% [bmim]Cl, although the protein remains in a

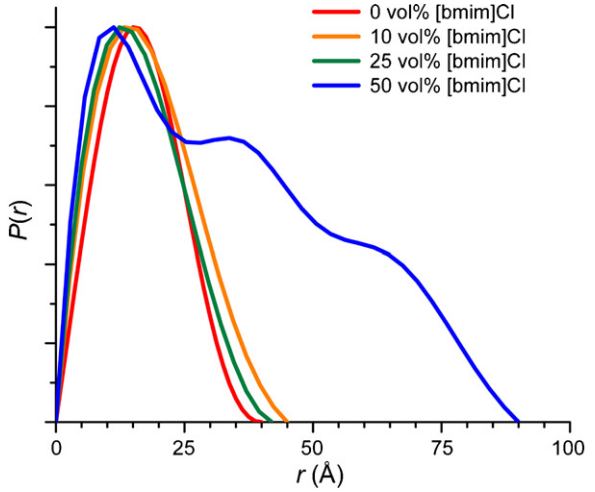

Fig. 3. $P(r)$ curves derived from the SANS data of cyt *c* shown in Fig. 2. The curves have been intensity-normalized to the same arbitrary value to facilitate comparison.

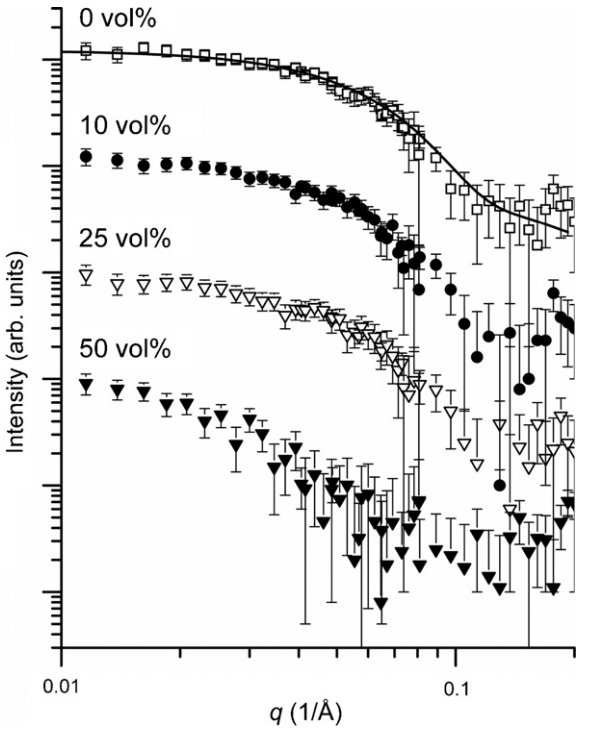

Fig. 4. SANS profiles of HSA in 0, 10, 25, and 50 vol.% aqueous [bmim]Cl. The solid curve shown is the model intensity profile calculated using ORNL_SAS [66] containing a 90%/10% monomer/dimer mixture calculated from the crystal structure of HSA [70] (PDB ID: 1AO6). The experimental curves have been offset for clarity.

near-native conformation. At the highest [bmim]Cl concentration employed (50 vol.%), the $P(r)$ of cyt *c* becomes rod-like with an R_g consistent with a previous study of guanidine hydrochloride denatured cyt *c* [58]. The drop in $I(0)$, also shown in Table 1, is consistent with the expected decrease based on the reduced differential scattering length density between the protein and solvent blank with increasing [bmim]Cl for samples collected at fixed protein concentration. Uncertainties in the 50 vol.% [bmim]Cl data set, arising from this diminished contrast, do not allow for an unambiguous conclusion, however. Previous work by one of the authors, in explanation of anomalous dye precipitation-to-redissolution behavior as [bmim][BF_4] was progressively added to water, has suggested that at lower levels the water-miscible [bmim][BF_4] plays the role of simple salt electrolyte, whereas highly concentrated [bmim][BF_4] solutions (≥25 wt%) behave more classically as co-solvents [69]. The current results are consistent with this view in that they show that when the [bmim]Cl salt is present at a solute quantity in aqueous solution it produces only a slight protein destabilization, whereas the presence of a significant co-solvent fraction leads to a substantial unfolding of cyt *c* molecules.

The series of SANS intensity profiles collected for HSA in aqueous solutions of [bmim]Cl is shown in Fig. 4, and the related $P(r)$ curves derived from fitting the data with GNOM [65] are revealed in Fig. 5. The trend in the data is rather similar to what was observed above for the cyt *c* samples, as can be seen in Table 2. The R_g and $P(r)$ data of the IL-free solution are consistent with a solution

Table 2
Structural parameters derived from SANS data of HAS.

Vol.% [bmim]Cl	R_g (Å)	d_{max} (Å)	$I(0)/I_{0\%}(0)$ (meas.)	$I(0)/I_{0\%}(0)$ (calc.)
0	30.0 ± 0.9	80	1.00	1.00
10	36.4 ± 2.6	120	0.96 ± 0.07	0.88
25	37.2 ± 2.9	125	0.72 ± 0.08	0.71
50	73.9 ± 6.9	225	0.85 ± 0.13	0.46

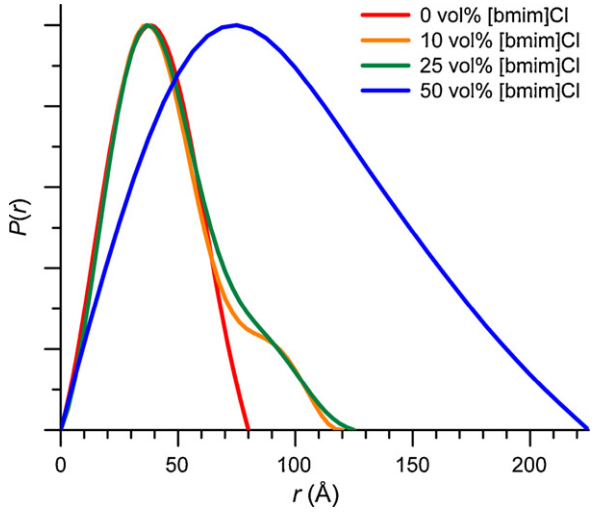

Fig. 5. $P(r)$ curves derived from the SANS data for HSA provided in Fig. 4. The curves have been scaled for clarity such that the major peaks retain the same value.

mainly comprised of HSA monomers with ~10% dimers present. This slight aggregation does not affect the results presented here. The fit line in Fig. 4 is a superposition of intensity profiles calculated from the high-resolution structure of the monomer (PDB ID: 1AO6) and the dimer from the crystal structure [70] using ORNL_SAS [66]. The R_g increases with increasing [bmim]Cl content, suggesting possible partially expanded intermediate states, although the effect remains subtle at 10 and 25 vol.% [bmim]Cl. By 50 vol.% [bmim]Cl, however, the effect on the solution structure of HSA is quite dramatic, with R_g more than doubling. Whereas the $P(r)$ curves suggest that the protein molecules adopt a slightly more open structure in response to [bmim]Cl levels at or below 25 vol.%, the $P(r)$ curve for the 50 vol.% [bmim]Cl sample suggests that the particle is actually globular, rather than rod-like as was observed for cyt *c*. The trend in $I(0)$ demonstrates that the HSA is not simply unfolding as the [bmim]Cl content within the solution rises. Instead, the relative $I(0)$ values evidence that HSA in fact oligomerizes in response to high concentrations of [bmim]Cl, with the state in the 50 vol.% [bmim]Cl solution being, in fact, a dimer on average. This oligomerization is supported by the globular structure implied by the $P(r)$ fitting. The SAXS data collected of HSA in aqueous mixtures of the same IL (not shown) support an unfolding of the protein. Interestingly, there is a nontrivial difference between the SANS and SAXS data collected for HSA in 50 vol.% [bmim]Cl. The SANS data at 50 vol.% [bmim]Cl presents a negative curvature, while the log–log plot of the SAXS data (not shown) is much more linear. A power-law fit of the data yields an exponent of −1.5, which is nearly the slope expected for a self-avoiding chain (−5/3) [71]. As stated earlier, HSA has an extensive network of disulfide bonds [70]. While neutrons cause essentially no radiation damage to biological samples of this nature, X-rays are capable of breaking bonds, including disulfide linkages. Consequently, the stabilizing network may have been disrupted during the SAXS measurements by radiation damage, allowing the protein to adopt a more truly denatured state.

The results presented here demonstrate that [bmim]Cl is a protein denaturant when in aqueous solution, chiefly at significant (co-solvent) levels. In the case of cyt *c*, the impact on the local environment at the heme group is perturbed much as it is by urea [61]. The limited impact of 10 vol.% [bmim]Cl on the Soret CD band of cyt *c* parallels earlier thermostability studies on ribonuclease A in aqueous [emim]Cl mixtures where [emim]Cl concentrations below 1.0 M were found to produce relatively little destabilization [46]. Because their study was restricted to concentrations ≤1.0 M, for this particular IL, direct molar comparison with our 50 vol.% [bmim]Cl (~3.1 M) sample is not feasible. Nonetheless, our SANS results show that the protein retains much of its global structure up to 25 vol.% [bmim]Cl, but unfolds at higher concentration while remaining predominantly monomeric. At the lower IL concentrations studied, the cyt *c* structure does not expand into a molten globule state, although the environment of the heme is clearly altered at 25 vol.% [bmim]Cl. The extension of the cyt *c* structure in 50 vol.% [bmim]Cl is similar to what occurs for the acid-unfolded state [56], the guanidine hydrochloride-unfolded state [58,59,72], and the unfolded state driven by urea [59].

Aqueous [bmim]Cl both denatures HSA and causes it to oligomerize in a manner consistent with dimerization. The denaturation of HSA has been studied in painstaking detail by a number of research groups employing a host of spectroscopic methods from optical rotation to static and time-resolved luminescence; this is exemplified in work from Wallevik [73], Muzammil et al. [74], and Flora et al. [75]. It is known that guanidine hydrochloride has a minimal impact on the secondary structure of HSA at concentrations up to ~1.5 M near neutral pH. Above this concentration, the response of the secondary structure of the protein to the denaturant increases sharply before leveling off near 6.0 M guanidine hydrochloride. 25 vol.% [bmim]Cl is roughly 1.5 M, so the response of HSA to these two ionic materials appears to be very similar despite their vastly different cations. A recent SANS study of bovine serum albumin (BSA) found that the protein began to unfold above 4.0 M urea, yet remained predominantly monomeric [55]. While the current results suggest that [bmim]Cl is a stronger denaturant of serum albumins than urea, the R_g of the fully unfolded state of BSA was found to be 94 Å, suggesting that either the unfolding by urea is more complete, or the [bmim]Cl-driven oligomerization of HSA results in a more compact state due to interactions between the polypeptide chains. Further experiments are required to flesh out these details.

4. Conclusions

This work demonstrates that aqueous mixtures of the IL [bmim]Cl influence the solution structures of the two archetype proteins cyt *c* and HSA in unique and concentration-dependent ways. In both cases, the water-miscible [bmim]Cl behaves much like the chaotropic agents urea or guanidine hydrochloride, in that high concentrations are required in order to denature the protein into a fully unfolded state. However, in contrast to these compounds, [bmim]Cl exhibits control over the oligomerization state of these proteins in a manner reliant upon the specific protein under consideration. Specifically, equine heart cyt *c* appears to remain exclusively monomeric in solution, whereas high concentrations of [bmim]Cl evidently drive the oligomerization of HSA. In this respect, [bmim]Cl influences HSA differently than elevated molar concentrations of either urea or guanidine hydrochloride.

In closing, it is important to note that IL components may affect the burial of nonpolar surfaces, main-chain hydrogen bonding, salt-bridge networks, conformational disorder at high temperatures, preservation of the essential water shell, and active-site flexibility within biological macromolecules. The ability of SANS to elucidate subtle changes in biomolecular geometry *in situ* should aid researchers in understanding how ILs impact the solution structure of enzymes. Forthcoming work from our groups will seek to extend these methods to include the study of ILs containing more "biocompatible" ions.

Acknowledgements

The authors thank Dr. Hugh M. O'Neill for access to the CD instrument used in this work. This work was supported by a Wigner Fellowship of Oak Ridge National Laboratory and by Project

KP1102010 of the Office of Biological and Environmental Research of the U.S. Department of Energy, under contract no. DE-AC05-00OR22725 with Oak Ridge National Laboratory, managed and operated by UT-Batelle, LLC.

References

[1] A. Lu, L.N. Zhang, Advance in solvents of cellulose, Acta Polym. Sin. (2007) 937–944.
[2] I.T. Horvath, P.T. Anastas, Innovations and green chemistry, Chem. Rev. 107 (2007) 2169–2173.
[3] F. van Rantwijk, R.A. Sheldon, Biocatalysis in ionic liquids, Chem. Rev. 107 (2007) 2757–2785.
[4] C.M. Gordon, New developments in catalysis using ionic liquids, Appl. Catal. A: Gen. 222 (2001) 101–117.
[5] U. Kragl, M. Eckstein, N. Kaftzik, Enzyme catalysis in ionic liquids, Curr. Opin. Biotechnol. 13 (2002) 565–571.
[6] R.A. Sheldon, R.M. Lau, M.J. Sorgedrager, F. van Rantwijk, K.R. Seddon, Biocatalysis in ionic liquids, Green Chem. 4 (2002) 147–151.
[7] R.A. Sheldon, F. van Rantwijk, R.M. Lau, in Ionic Liquids as Green Solvents: Progress and Prospects; Rogers, R.D., Seddon, K.R., Eds.; ACS Symposium Series 856; American Chemical Society: Washington, DC, 2003, pp. 192–205.
[8] F. van Rantwijk, R.M. Lau, R.A. Sheldon, Biocatalytic transformations in ionic liquids, Trends Biotechnol. 21 (2003) 131–138.
[9] Q.B. Liu, Z.H. Zhang, F.J. Zhang, Progress in biocatalytic reactions in ionic liquids, Prog. Chem. 17 (2005) 1060–1066.
[10] Z. Yang, W.B. Pan, Ionic liquids: green solvents for nonaqueous biocatalysis, Enzyme Microb. Technol. 37 (2005) 19–28.
[11] Y.H. Moon, S.M. Lee, S.H. Ha, Y.M. Koo, Enzyme-catalyzed reactions in ionic liquids, Korean J. Chem. Eng. 23 (2006) 247–263.
[12] G.A. Baker, S.N. Baker, S. Pandey, F.V. Bright, An analytical view of ionic liquids, Analyst 130 (2005) 800–808.
[13] K.W. Kim, B. Song, M.Y. Choi, M.J. Kim, Biocatalysis in ionic liquids: markedly enhanced enantioselectivity of lipase, Org. Lett. 3 (2001) 1507–1509.
[14] M. Eckstein, P. Wasserscheid, U. Kragl, Enhanced enantioselectivity of lipase from *Pseudomonas* sp. at high temperatures and fixed water activity in the ionic liquid, 1-butyl-3-methylimidazolium bis[(trifluoromethyl)sulfonyl]amide, Biotechnol. Lett. 24 (2002) 763–767.
[15] W.Y. Lou, M.H. Zong, H. Wu, R. Xu, J.F. Wang, Markedly improving lipase-mediated asymmetric ammonolysis of D,L-*p*-hydroxyphenylglycine methyl ester by using an ionic liquid as the reaction medium, Green Chem. 7 (2005) 500–506.
[16] J.Y. Xin, Y.J. Zhao, Y.G. Shi, C.G. Xia, S.B. Li, Enantioselective hydrolysis of naproxen methyl ester by lipase in a water-saturated ionic liquid, Chin. J. Catal. 26 (2005) 118–122.
[17] D. Barahona, P.H. Pfromm, M.E. Rezac, Effect of water activity on the lipase catalyzed esterification of geraniol in ionic liquid [bmim]PF_6, Biotechnol. Bioeng. 93 (2006) 318–324.
[18] Z.G. Chen, M.H. Zong, G.J. Li, Lipase-catalyzed acylation of konjac glucomannan in ionic liquids, J. Chem. Technol. Biotechnol. 81 (2006) 1225–1231.
[19] Z. Guo, X.B. Xu, Lipase-catalyzed glycerolysis of fats and oils in ionic liquids: a further study on the reaction system, Green Chem. 8 (2006) 54–62.
[20] K. Nakashima, J. Okada, T. Maruyama, N. Kamiya, M. Goto, Activation of lipase in ionic liquids by modification with comb-shaped poly(ethylene glycol), Sci. Technol. Adv. Mater. 7 (2006) 692–698.
[21] F. van Rantwijk, F. Secundo, R.A. Sheldon, Structure and activity of *Candida antarctica* lipase B in ionic liquids, Green Chem. 8 (2006) 282–286.
[22] Y. Yi, B. Shu, S. Yan, Comparison of lipase-catalyzed enantio selective esterification of (+/−)-menthol in ionic liquids and organic solvents, Food Chem. 97 (2006) 324–330.
[23] S.H. Ha, M.N. Lan, S.H. Lee, S.M. Hwang, Y.M. Koo, Lipase-catalyzed biodiesel production from soybean oil in ionic liquids, Enzyme Microb. Technol. 41 (2007) 480–483.
[24] F.J. Hernandez-Fernandez, A.P. de los Rios, M. Rubio, D. Gomez, G. Villora, Enhancement of activity and selectivity in lipase-catalyzed transesterification in ionic liquids by the use of additives, J. Chem. Technol. Biotechnol. 82 (2007) 882–887.
[25] M.H. Katsoura, A.C. Polydera, P. Katapodis, F.N. Kolisis, H. Stamatis, Effect of different reaction parameters on the lipase-catalyzed selective acylation of polyhydroxylated natural compounds in ionic liquids, Process Biochem. 42 (2007) 1326–1334.
[26] S. Shah, M.N. Gupta, Kinetic resolution of (+/−)-1-phenylethanol in [Bmim][PF6] using high activity preparations of lipases, Bioorg. Med. Chem. Lett. 17 (2007) 921–924.
[27] S.H. Lee, D.T. Dang, S.H. Ha, W.J. Chang, Y.M. Koo, Lipase-catalyzed synthesis of fatty acid sugar ester using extremely supersaturated sugar solution in ionic liquids, Biotechnol. Bioeng. 99 (2008) 1–8.
[28] N. Li, D. Ma, M.H. Zong, Enhancing the activity and regioselectivity of lipases for 3′-benzoylation of floxuridine and its analogs by using ionic liquid-containing systems, J. Biotechnol. 133 (2008) 103–109.
[29] H. Zhao, G.A. Baker, Z.Y. Song, O. Olubajo, T. Crittle, D. Peters, Designing enzyme-compatible ionic liquids that can dissolve carbohydrates, Green Chem. 10 (2008) 696–705.
[30] J.A. Laszlo, D.L. Compton, Alpha-chymotrypsin catalysis in imidazolium-based ionic liquids, Biotechnol. Bioeng. 75 (2001) 181–186.
[31] P. Lozano, T. de Diego, J.P. Guegan, M. Vaultier, J.L. Iborra, Stabilization of alpha-chymotrypsin by ionic liquids in transesterification reactions, Biotechnol. Bioeng. 75 (2001) 563–569.
[32] M.F. Machado, J.M. Saraiva, Thermal stability and activity regain of horseradish peroxidase in aqueous mixtures of imidazolium-based ionic liquids, Biotechnol. Lett. 27 (2005) 1233–1239.
[33] D. Das, A. Dasgupta, P.K. Das, Improved activity of horseradish peroxidase (HRP) in 'specifically designed' ionic liquid, Tetrahedron Lett. 48 (2007) 5635–5639.
[34] S.F. Wang, T. Chen, Z.L. Zhang, D.W. Pang, Activity and stability of horseradish peroxidase in hydrophilic room temperature ionic liquid and its application in non-aqueous biosensing, Electrochem. Commun. 9 (2007) 1337–1342.
[35] W.Y. Lou, M.H. Zong, H. Wu, Enhanced activity, enantioselectivity and stability of papain in asymmetric hydrolysis of D,L-*p*-hydroxyphenylglycine methyl ester with ionic liquid, Biocatal. Biotransform. 22 (2004) 171–176.
[36] W.Y. Lou, M.H. Zong, T.J. Smith, H. Wu, J.F. Wang, Impact of ionic liquids on papain: an investigation of structure–function relationships, Green Chem. 8 (2006) 509–512.
[37] J.A. Laszlo, D.L. Compton, Comparison of peroxidase activities of hemin, cytochrome *c* and microperoxidase-11 in molecular solvents and imidazolium-based ionic liquids, J. Mol. Catal. B: Enzym. 18 (2002) 109–120.
[38] K.L. Tee, D. Roccatano, S. Stolte, J. Arning, J. Bernd, U. Schwaneberg, Ionic liquid effects on the activity of monooxygenase P450BM-3, Green Chem. 10 (2008) 117–123.
[39] K. Fujita, D.R. MacFarlane, M. Forsyth, Protein solubilising and stabilising ionic liquids, Chem. Commun. (2005) 4804–4806.
[40] Z. Yang, Y.J. Yue, M. Xing, Tyrosinase activity in ionic liquids, Biotechnol. Lett. 30 (2008) 153–158.
[41] S.N. Baker, E.B. Brauns, T.M. McCleskey, A.K. Burrell, G.A. Baker, Fluorescence quenching immunoassay performed in an ionic liquid, Chem. Commun. (2006) 2851–2853.
[42] S.N. Baker, T.M. McCleskey, S. Pandey, G.A. Baker, Fluorescence studies of protein thermostability in ionic liquids, Chem. Commun. (2004) 940–941.
[43] T. De Diego, P. Lozano, S. Gmouh, M. Vaultier, J.L. Iborra, Understanding structure—stability relationships of *Candida antartica* lipase B in ionic liquids, Biomacromolecules 6 (2005) 1457–1464.
[44] T. De Diego, P. Lozano, S. Gmouh, M. Vaultier, J.L. Iborra, Fluorescence and CD spectroscopic analysis of the alpha-chymotrypsin stabilization by the ionic liquid, 1-ethyl-3-methylimidazolium bis[(trifluoromethyl)sulfonyl]amide, Biotechnol. Bioeng. 88 (2004) 916–924.
[45] D. Sate, M.H.A. Janssen, G. Stephens, R.A. Sheldon, K.R. Seddon, J.R. Lu, Enzyme aggregation in ionic liquids studied by dynamic light scattering and small angle neutron scattering, Green Chem. 9 (2007) 859–867.
[46] D. Constantinescu, H. Weingärtner, C. Herrmann, Protein denaturation by ionic liquids and the Hofmeister series: a case study of aqueous solutions of ribonuclease A, Angew. Chem. Int. Ed. 46 (2007) 8887–8889.
[47] H. Zhao, Effect of ions and other compatible solutes on enzyme activity, and its implication for biocatalysis using ionic liquids, J. Mol. Catal. B 37 (2005) 16–25.
[48] H. Jin, B. O'Hare, J. Dong, S. Arzhantsev, G.A. Baker, J.F. Wishart, A.J. Benesi, M. Maroncelli, Physical properties of ionic liquids consisting of the 1-butyl-3-methylimidazolium cation with various anions and the bis(trifluoromethylsulfonyl)imide anion with various cations, J. Phys. Chem. B 112 (2008) 81–92.
[49] T.A. McCarty, P.M. Page, G.A. Baker, F.V. Bright, Behavior of acrylodan-labeled human serum albumin dissolved in ionic liquids, Ind. Eng. Chem. Res. 47 (2008) 560–569.
[50] N. Byrne, L.M. Wang, J.P. Belieres, C.A. Angell, Reversible folding–unfolding, aggregation protection, and multi-year stabilization, in high concentration protein solutions, using ionic liquids, Chem. Commun. (2007) 2714–2716.
[51] D.I. Svergun, M.H.J. Koch, Small-angle scattering studies of biological macromolecules in solution, Rep. Prog. Phys. 66 (2003) 1735–1782.
[52] X.H. Guo, N.M. Zhao, S.H. Chen, J. Teixeira, Small-angle neutron-scattering study of the structure of protein detergent complexes, Biopolymers 29 (1990) 335–346.
[53] A. Das, R. Chitra, R.R. Choudhury, M. Ramanadham, Structural changes during the unfolding of bovine serum albumin in the presence of urea: a small-angle neutron scattering study, Pramana-J. Phys. 63 (2004) 363–368.
[54] C.T. Lee, K.A. Smith, T.A. Hatton, Photocontrol of protein folding: the interaction of photosensitive surfactants with bovine serum albumin, Biochemistry 44 (2005) 524–536.
[55] S. Chodankar, V.K. Aswal, J. Kohlbrecher, R. Vavrin, A.G. Wagh, Structural evolution during protein denaturation as induced by different methods, Phys. Rev. E 77 (2008).
[56] M. Kataoka, Y. Hagihara, K. Mihara, Y. Goto, Molten globule of cytochrome *c* studied by small-angle X-ray scattering, J. Mol. Biol. 229 (1993) 591–596.
[57] D. Hamada, Y. Kuroda, M. Kataoka, S. Aimoto, T. Yoshimura, Y. Goto, Role of heme axial ligands in the conformational stability of the native and molten globule states of horse cytochrome *c*, J. Mol. Biol 256 (1996) 172–186.
[58] D.J. Segel, A.L. Fink, K.O. Hodgson, S. Doniach, Protein denaturation: a small-angle X-ray scattering study of the ensemble of unfolded states of cytochrome *c*, Biochemistry 37 (1998) 12443–12451.
[59] Y.J. Shiu, U.S. Jeng, C. Su, Y.S. Huang, M. Hayashi, K.K. Liang, Y.L. Yeh, S.H. Lin, A modified Ising model for the thermodynamic properties of local and global protein folding unfolding observed by circular dichroism and small-angle X-ray scattering, J. Appl. Crystallogr. 40 (2007) S195–S199.
[60] I.J. Hsu, Y.J. Shiu, U.S. Jeng, T.H. Chen, Y.S. Huang, Y.H. Lai, L.N. Tsai, L.Y. Jang, J.F. Lee, L.J. Lin, S.H. Lin, Y. Wang, A solution study on the local and global structure

changes of cytochrome *c*: an unfolding process induced by urea, J. Phys. Chem. A 111 (2007) 9286–9290.
[61] Y.P. Myer, Conformation of cytochromes. 3. Effect of urea, temperature, extrinsic ligands, and pH variation on conformation of horse heart ferricytochrome *c*, Biochemistry 7 (1968) 765–776.
[62] W.E. Gardinier, G.A. Baker, S.N. Baker, F.V. Bright, Behavior of pyrene end-labeled poly(dimethylsiloxane) polymer tails in mixtures of 1-butyl-3-methylimidazolium bis(trifluoromethyl)sulfonylimide and toluene, Macromolecules 38 (2005) 8574–8582.
[63] A.K. Burrell, R.E. Del Sesto, S.N. Baker, T.M. McCleskey, G.A. Baker, The large scale synthesis of pure imidazolium and pyrrolidinium ionic liquids, Green Chem. 9 (2007) 449–454.
[64] J.D. Woodward, J.M. Pickel, L.M. Anovitz, W.T. Heller, A.J. Rondinone, Self-assembled colloidal crystals from ZrO_2 nanoparticles, J. Phys. Chem. B 110 (2006) 19456–19460.
[65] D.I. Svergun, Determination of the regularization parameter in indirect-transform methods using perceptual criteria, J. Appl. Crystallogr. 25 (1992) 495–503.
[66] E. Tjioe, W.T. Heller, ORNL_SAS: software for calculation of small-angle scattering intensities of proteins and protein complexes, J. Appl. Crystallogr. 40 (2007) 782–785.
[67] S.G. Sivakolundu, P.A. Mabrouk, Cytochrome *c* structure and redox function in mixed solvents are determined by the dielectric constant, J. Am. Chem. Soc. 122 (2000) 1513–1521.
[68] G.W. Bushnell, G.V. Louie, G.D. Brayer, High-resolution 3-dimensional structure of horse heart cytochrome *c*, J. Mol. Biol. 214 (1990) 585–595.
[69] M. Ali, G.A. Baker, S. Pandey, Dye redissolution after precipitation with a water-miscible ionic liquid, Chem. Lett. 37 (2008) 260–261.
[70] S. Sugio, A. Kashima, S. Mochizuki, M. Noda, K. Kobayashi, Crystal structure of human serum albumin at 2.5 angstrom resolution, Protein Eng. 12 (1999) 439–446.
[71] J.S. Pedersen, P. Schurtenberger, Scattering functions of semiflexible polymers with and without excluded volume effects, Macromolecules 29 (1996) 7602–7612.
[72] D. Hamada, M. Hoshino, M. Kataoka, A.L. Fink, Y. Goto, Intermediate conformational states of apocytochrome *c*, Biochemistry 32 (1993) 10351–10358.
[73] K. Wallevik, Reversible denaturation of human serum albumin by pH, temperature, and guanidine hydrochloride followed by optical-rotation, J. Biol. Chem. 248 (1973) 2650–2655.
[74] S. Muzammil, Y. Kumar, S. Tayyab, Molten globule-like state of human serum albumin at low pH, Eur. J. Biochem. 266 (1999) 26–32.
[75] K. Flora, J.D. Brennan, G.A. Baker, M.A. Doody, F.V. Bright, Unfolding of acrylodan-labeled human serum albumin probed by steady-state and time-resolved fluorescence methods, Biophys. J. 75 (1998) 1084–1096.